Phosphido-bridged iridium clusters: crystal and molecular structure of $[Ir_3(\mu\text{-}PPh_2)_3(\mu\text{-bis(diphenylphosphino)methane})(CO)_4]$ and correlation of Ir–Ir distances with valence electron count

Jane Browning, Keith R. Dixon* and Neil J. Meanwell
Department of Chemistry, University of Victoria, Victoria, BC, V8W 3P6 (Canada)

(Received March 30, 1993; revised May 27, 1993)

Abstract

The 46 electron cluster, $[Ir_3(\mu\text{-}PPh_2)_3(\mu\text{-dppm})(CO)_3]$ (**1**), dppm = bis(diphenylphosphino)methane, undergoes (reversible) addition of carbon monoxide to the 48 electron derivative, $[Ir_3(\mu\text{-}PPh_2)_3(\mu\text{-dppm})(CO)_4]$ (**2**). This product crystallizes in the $P\bar{1}$ space group ($Z=2$) with two molecules in the asymmetric unit and with unit cell parameters: $a=21.559(4)$, $b=22.337(4)$, $c=13.860(3)$ Å, $\alpha=89.05(2)$, $\beta=95.46(2)$, $\gamma=108.66(1)°$. The molecular structure consists of an iridium triangle with two edges bridged by roughly coplanar phosphorus atoms. The third edge is also bridged by phosphorus but approximately perpendicular to the Ir_3 plane. The unique Ir–Ir distance is 2.707(3) Å and the other distances average 2.989(3) Å. Comparison of the latter distance with corresponding distances in **1** and $[Ir_3(\mu\text{-}PPh_2)_3(CO)_5(t\text{-BuNC})_2]$ (**3**), shows a regular increase in Ir–Ir length, 2.805(2), 2.989(3), and 3.188 Å in **1**–**3**, respectively, as the valence electron count changes from 46 to 48 to 50 electrons. ^{31}P NMR data for the three molecules are also consistent with the changes in Ir–Ir distances.

Introduction

The group of trinuclear clusters based on a triangular $Rh_3(\mu\text{-}PPh_2)_3$ core constitutes an especially interesting example of metal atoms linked by strong yet flexible bridges [1–6]. In principle, such bridges are able to preserve the integrity of a complex while permitting the making and breaking of metal–metal bonds, and the rhodium triangles provide an important demonstration of this capability. For example, the 46 electron, pentacarbonyl cluster, $[Rh_3(\mu\text{-}PPh_2)_3(CO)_5]$, has Rh–Rh bonds which average 2.77 Å [2], whereas the related 50 electron, heptacarbonyl, $[Rh(\mu\text{-}PPh_2)_3(CO)_7]$, has essentially non-bonded metal–metal distances of 3.14 Å [6]. We have recently synthesized analogous complexes with an $Ir_3(\mu\text{-}PPh_2)_3$ core [7], and have shown that similar considerations apply: for example in $[Ir_3(\mu\text{-}PPh_2)_3(\mu\text{-dppm})(CO)_3]$ (**1**), dppm = bis(diphenylphosphino)methane, av. Ir–Ir = 2.78 Å, and in $[Ir_3(\mu\text{-}PPh_2)_3(CO)_5(t\text{-BuNC})_2]$ (**3**) av. Ir–Ir = 3.23 Å. The structures of **1**–**3** are shown in Scheme 1.

The literature contains several other structurally characterized $M_3(\mu\text{-}PPh_2)_3$ clusters, including examples with

*Author to whom correspondence should be addressed.

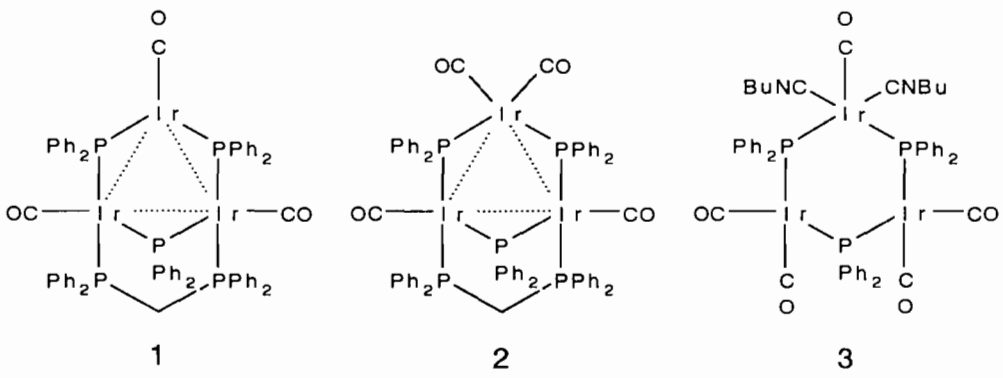

Scheme 1. Structures of compounds **1**–**3**.

0020-1693/93/$6.00

46 valence electrons: $[Rh_3(\mu\text{-}PPh_2)_3(CO)_3(PPh_3)_2]$ [1] and $[Ir_3(\mu\text{-}P(t\text{-}Bu)_2)_3(CO)_5]$ [8]; and with 50 valence electrons: $[Rh_3(\mu\text{-}PPh_2)_3(CO)_6(PHPh_2)]$ [4]. The M–M distances in these clusters average 2.78, 2.78 and 3.16 Å, respectively; confirming the generality of the relation between electron count and bond distance and posing an immediate question regarding possible 48 electron species. Despite this obvious potential interest in the structural parameters of the intermediate case, no examples of 48 electron clusters have been characterized. In the case of the rhodium triangles, addition of carbon monoxide to $[Rh_3(\mu\text{-}PPh_2)_3(CO)_5]$ yields an indeterminate material, $\{Rh(PPh_2)(CO)_x\}_n$, probably with $x=n=3$, but the only characterized product is the heptacarbonyl mentioned above [6]. In contrast, we now report that $[Ir_3(\mu\text{-}PPh_2)_3(\mu\text{-dppm})(CO)_3]$ undergoes simple (reversible) addition of carbon monoxide. The 48 electron, tetracarbonyl product, $[Ir_3(\mu\text{-}PPh_2)_3(\mu\text{-dppm})(CO)_4]$ (**2**), is sufficiently stable under a carbon monoxide atmosphere for full characterization and structural study by X-ray diffraction.

Experimental

Synthesis and spectroscopic studies

All operations were carried out under an atmosphere of dry nitrogen using standard Schlenk tube techniques. Solvents were dried by appropriate methods and distilled under nitrogen prior to use. The tricarbonyl cluster, $[Ir_3(\mu\text{-}PPh_2)_3(\mu\text{-dppm})(CO)_3]$ (**1**), was prepared as previously described [7]. Microanalysis was by the Canadian Microanalytical Service, Vancouver, BC, Canada. ^{31}P NMR spectra were recorded at 101.3 MHz, using a Bruker WM250 Fourier transform spectrometer. The solvent was CH_2Cl_2 and a lock signal was derived from the deuterium resonance of a capilliary insert containing C_6D_6. Protons were decoupled by broad band ('noise') irradiation, and chemical shifts were measured relative to external $P(OMe)_3$ and are reported in ppm relative to 85% H_3PO_4 using a conversion factor of +141 ppm. Positive chemical shifts are downfield of the reference.

$[Ir_3(\mu\text{-}PPh_2)_3(\mu\text{-dppm})(CO)_4]$ (2)

Carbon monoxide was bubbled vigorously for 5 min through a solution of **1** (0.040 g, 0.025 mmol) in dichloromethane (4 ml). The resulting deep red solution was carefully layered with hexane (15 ml) under an atmosphere of carbon monoxide to yield **2** as dark red crystals (0.030 g, 0.018 mmol). IR (cm^{-1} in KBr): $\nu(CO)$ = 1915s br, 1875m br. *Anal.* Calc. for $C_{65}H_{52}O_4P_5Ir_3$: C, 47.9; H, 3.22. Found: C, 47.5; H, 3.16%.

When crystals of **2** were redissolved in dichloromethane (5 ml), a ^{31}P NMR spectrum of the solution showed the tri and tetracarbonyl clusters, **1** and **2**, to be present in approximately equal quantities. After purging the solution with nitrogen for 1 h the spectrum showed only the tricarbonyl and bubbling carbon monoxide through this solution completely regenerated the tetracarbonyl.

X-ray data collection

A crystal of **2** suitable for study by X-ray diffraction was grown as described above. Preliminary photographic work was carried out with Weissenberg and precession cameras using Cu Kα radiation. After establishment of symmetry and approximate unit cells the crystal was transferred to an Enraf-Nonius CAD4 diffractometer and the unit cell refined by least-squares methods employing pairs of centering measurements. Diffraction data were collected using the NRCCAD modification of the ENRAF-NONIUS program [9] and the 'Profile' $\omega/2\theta$ scan developed by Grant and Gabe [10]. Three standard reflections were measured every hour to check crystal stability and three others were measured every 400 reflections to check crystal orientation. There was evidence of about 20% decomposition of the crystal during data collection. Lorentz and polarization factors were applied and the data were corrected for absorption using an empirical method based on the work of North *et al.* [11] as implemented in the CAD4 structure determining package.

Structure solution and refinement

The structure was found and refined using the SHELX-76 program package [12] and illustrations were drawn using ORTEP [13]. The atomic scattering factors used were for neutral atoms, with corrections for anomalous dispersion [14]. The structure was solved by direct methods, developed by standard Fourier synthesis procedures using difference maps, and refined by the method of least-squares minimizing $\Sigma w\Delta^2$ where $\Delta = ||F_o| - |F_c||$. The weights were obtained from counting statistics using $w = 1/\sigma^2(F) + 0.001F^2)$. The iridium atoms were treated anisotropically, all others isotropically, and the phenyl rings were refined as rigid groups. Hydrogen atoms were not located but the final difference maps gave no indication that any material had been overlooked.

Results and discussion

The $^{31}P\{^1H\}$ nuclear magnetic resonance spectrum of **1** in dichloromethane consists of a triplet of triplets and two doublets, due to the unique phosphorus bridge (P(2) in Scheme 2), the other phosphorus bridges, P(1,3)* and the dppm ligand, P(4,5) respectively. When this solution is saturated with carbon monoxide, the

*This numbering is chosen to conform with the X-ray structure. For NMR purposes it is slightly unconventional (see Scheme 2).

TABLE 1. ^{31}P NMR[a] chemical shifts (ppm) and coupling constants (Hz)

	δ(1,3)	δ(2)	δ(4,5)	J(1,2)	J(2,4)
$[Ir_3(\mu\text{-}PPh_2)_3(CO)_5]$[b]	+240.5	+100.5		15	
$[Ir_3(\mu\text{-}PPh_2)_3(\mu\text{-dppm})(CO)_3]$ (1)	+241.7	+119.3	−14.9	24	169
$[Ir_3(\mu\text{-}PPh_2)_3(CO)_6]$[b]	+179.8	+179.8		[d]	
$[Ir_3(\mu\text{-}PPh_2)_3(\mu\text{-dppm})(CO)_4]$ (2)	+201.9	+143.6	−21.6	26	194
$[Ir_3(\mu\text{-}PPh_2)_3(CO)_5(t\text{-BuNC})_2]$ (3)[c]	−8.2	+38.0		149	

[a]For convenience, the atom labelling scheme is the same as that used for the X-ray structures (Scheme 2). Since P(1),P(3) and P(4),P(5) are chemically equivalent pairs, P(3) and P(5) are more properly labelled P(1′) and P(4′) for NMR purposes. All unlisted couplings were less than the spectrum resolution of about 5 Hz. [b]Data from ref. 7. Note that the data in this reference were inadvertently referenced to trimethyl phosphite rather than the phosphoric acid reference used here. [c]^{31}P NMR parameters for this molecule were reported in ref. 7. However, subsequent experiments have shown that the sample used was contaminated with excess t-BuNC and consisted mainly of $[Ir_3(\mu\text{-}PPh_2)_3(CO)_4(t\text{-BuNC})_3]$. This Table gives corrected parameters for $[Ir_3(\mu\text{-}PPh_2)_3(CO)_5(t\text{-BuNC})_2]$. [d]Not available from observed spectrum.

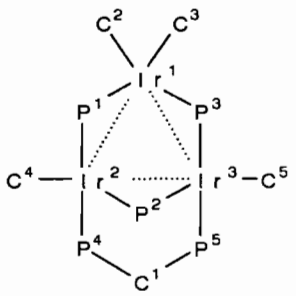

Scheme 2. Atom labelling scheme for Tables 1–3 and 'Discussion'. Note that for NMR purposes P(3) and P(5) would be more correctly labelled P(1′) and P(4′).

basic pattern remains unchanged but significant changes in the coupling constants and chemical shifts (Table 1) indicate formation of a new compound. Careful crystallization under an atmosphere of carbon monoxide gives dark red crystals of **2**. In solution, interconversion of **1** and **2** is labile and repeatable by alternate saturation with carbon monoxide or purging with nitrogen.

Table 1 shows that the P(1,3) bridges of $[Ir_3(\mu\text{-}PPh_2)_3(CO)_5]$, +240.5 ppm, are dramatically shielded when two isocyanide groups are added to form **3**, −8.2 ppm. This is normal behaviour for phosphido groups bridging two metals in the presence and absence of metal–metal bonds [15, 16], and in the present case the reaction is accompanied by expansion of the Ir(1)–Ir(2,3) distances from about 2.8 Å (based on the Rh analogue) to 3.19 Å [7]. The increase in shielding at the unique bridge, P(2), is smaller but significant, from +100.5 to +38.0 ppm as the associated Ir(2)–Ir(3) distance changes from 2.7 to 3.33 Å. The other important structural change is that the P(2) bridge, initially roughly perpendicular to the Ir_3–P(1)–P(3) plane in $[Ir_3(\mu\text{-}PPh_2)_3(CO)_5]$, becomes coplanar in **3**. In NMR, this change is accompanied by an increase in J(1,2) from 15 to 149 Hz. When a single CO is added to **1** to form **2** the changes are less dramatic. The two equivalent bridges, P(1,3), are more shielded (Table 1), but only from +241.7 to +201.9 ppm, and the coupling to the unique bridge, J(1,2) 26 Hz, changes hardly at all. This suggests that there has been some lengthening of the Ir(1)–Ir(2,3) distances but that the P(2) bridge has not moved into the Ir_3–P(1)–P(3) plane; conclusions which are confirmed by the X-ray structure reported below. The chemical shift of P(2) is also consistent with the X-ray results, since it is slightly deshielded relative to **1**, +143.6 compared to +119.3 ppm, and the associated Ir(2)–Ir(3) bond length is shorter in **2**, 2.71 compared to 2.74 Å.

X-ray structures

Compound **2** crystallizes in the $P\bar{1}$ space group with 2 molecules in the asymmetric unit, producing a very large X-ray structural problem. One of the two molecules of the asymmetric unit is shown as an ORTEP diagram in Fig. 1. The other molecule is similar except for minor

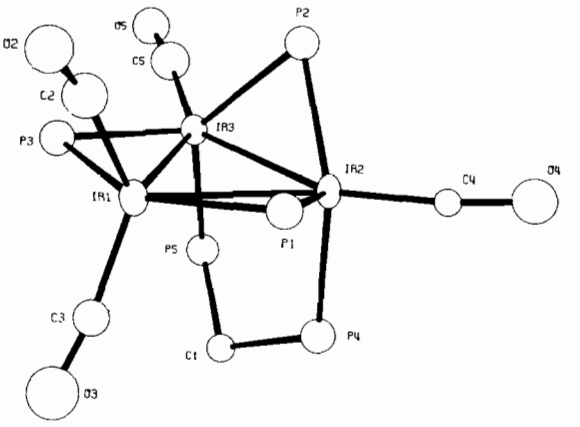

Fig. 1. ORTEP plot of one molecule of $[Ir_3(\mu\text{-}PPh_2)_3(\mu\text{-dppm})(CO)_4]$ (**2**). The two phenyl rings attached to each phosphorus are not shown.

conformational changes, presumably induced by crystal packing forces. Unit cell and other parameters related to the crystal structure determination are in Table 2. Selected bond lengths and angles are shown in Tables 3 and 4 for both molecules (A and B) of the asymmetric unit. The atom labels are shown in Scheme 2 and the Tables also include comparison data for **1** and **3**. To simplify the presentation, structural parameters of **2**

TABLE 2. Selected crystallographic data for $[Ir_3(\mu\text{-}PPh_2)_3(\mu\text{-}dppm)(CO)_4]$ (**2**)

Formula	$C_{65}H_{52}O_4P_5Ir_3$
Formula weight	1628.66
Space group	$P\bar{1}$ (No. 2)
a (Å)	21.559(4)
b (Å)	22.337(4)
c (Å)	13.860(3)
α (°)	89.05(2)
β (°)	95.46(2)
γ (°)	108.66(1)
V (Å^3)	6294
Z	2
Diffractometer	Enraf-Nonius CAD4
Radiation (λ, Å)	Cu Kα (1.542)
Monochromator	Zr filter
μ (cm^{-1})	124.61
No. observed reflections ($I > 2\sigma(I)$)	6827
R	0.096
R_w	0.108

$R = (\Sigma\Delta/\Sigma F_o)$; $R_w = (\Sigma w\Delta^2/\Sigma wF_o^2)^{1/2}$. $w = 1/(\sigma^2(F) + 0.001F^2)$; $\Delta = ||F_o| - |F_c||$.

TABLE 3. Selected interatomic distances[a] (Å) for $[Ir_3(\mu\text{-}PPh_2)_3(\mu\text{-}dppm)(CO)_3]$ (**1**), $[Ir_3(\mu\text{-}PPh_2)_3(\mu\text{-}dppm)(CO)_4]$ (**2**) and $[Ir_3(\mu\text{-}PPh_2)_3(CO)_5(t\text{-}BuNC)_2]$ (**3**)

	1[b]	2A	2B	3[b]
Ir(1)–Ir(2)	2.805(2)	3.011(3)	2.980(3)	3.176(2)
Ir(1)–Ir(3)	2.805(2)	3.035(2)	2.929(3)	3.199(2)
Ir(1)–P(1)	2.270(8)	2.290(13)	2.322(11)	2.373(7)
Ir(1)–P(3)	2.270(8)	2.286(13)	2.331(11)	2.378(7)
Ir(1)–C(2)	1.74(6)	1.82(4)	1.74(4)	1.80(4)
Ir(1)–C(3)		1.95(5)	2.02(8)	
Ir(2)–Ir(3)	2.744(3)	2.703(3)	2.711(3)	3.329(2)
Ir(2)–P(1)	2.289(8)	2.258(11)	2.290(12)	2.273(7)
Ir(2)–P(2)	2.292(10)	2.323(10)	2.283(13)	2.321(7)
Ir(2)–P(4)	2.327(9)	2.361(12)	2.333(13)	1.77(3)
Ir(2)–C(4)	1.77(4)	1.72(4)	1.87(4)	1.86(4)
Ir(3)–P(2)	2.292(10)	2.307(14)	2.305(11)	2.332(7)
Ir(3)–P(3)	2.289(8)	2.279(11)	2.261(13)	2.300(8)
Ir(3)–P(5)	2.327(9)	2.320(12)	2.352(12)	1.93(4)
Ir(3)–C(5)	1.77(4)	1.81(5)	1.88(4)	1.87(4)
P(4)–C(1)	1.85(3)	1.85(4)	1.82(3)	
P(5)–C(1)	1.85(3)	1.83(3)	1.91(4)	
O(2)–C(2)	1.29(6)	1.19(6)	1.15(7)	1.16(5)
O(3)–C(3)		1.08(6)	1.07(9)	
O(4)–C(4)	1.23(4)	1.24(5)	1.16(5)	1.18(4)
O(5)–C(5)	1.23(4)	1.14(6)	1.14(5)	1.16(5)

[a]e.s.d.s are given in parentheses. [b]Data from ref. 7.

TABLE 4. Selected bond angles[a] (°) for $[Ir_3(\mu\text{-}PPh_2)_3(\mu\text{-}dppm)(CO)_3]$ (**1**), $[Ir_3(\mu\text{-}PPh_2)_3(\mu\text{-}dppm)(CO)_4]$ (**2**) and $[Ir_3(\mu\text{-}PPh_2)_3(CO)_5(t\text{-}BuNC)_2]$ (**3**)

	1[b]	2A	2B	3[b]
Ir(2)–Ir(1)–Ir(3)	58.6(1)	53.1(1)	54.6(1)	63.0(1)
Ir(2)–Ir(1)–P(1)	52.3(2)	48.1(3)	49.3(3)	45.6(2)
Ir(2)–Ir(1)–P(3)	110.4(2)	101.3(3)	102.8(3)	108.8(2)
Ir(2)–Ir(1)–C(2)	150.6(2)	109.7(12)	107.5(18)	147.7(11)
Ir(2)–Ir(1)–C(3)		119.7(15)	102.8(18)	
Ir(3)–Ir(1)–P(1)	110.4(2)	99.7(3)	103.7(3)	108.5(2)
Ir(3)–Ir(1)–P(3)	52.3(2)	48.2(3)	49.3(3)	45.8(2)
Ir(3)–Ir(1)–C(2)	150.6(2)	115.0(13)	102.0(16)	148.6(11)
Ir(3)–Ir(1)–C(3)		111.6(12)	110.0(18)	
P(1)–Ir(1)–P(3)	157.7(4)	146.2(4)	151.5(4)	154.3(3)
P(1)–Ir(1)–C(2)	99.0(3)	102.9(15)	95.9(15)	102.4(11)
P(1)–Ir(1)–C(3)		94.7(16)	90.5(18)	
P(3)–Ir(1)–C(2)	99.0(3)	101.5(15)	98.8(14)	103.3(11)
P(3)–Ir(1)–C(3)		89.6(15)	91.3(18)	
C(2)–Ir(1)–C(3)		126(2)	145(3)	
Ir(1)–Ir(2)–Ir(3)	60.7(1)	63.9(1)	61.7(1)	58.8(1)
Ir(1)–Ir(2)–P(1)	51.7(2)	49.0(3)	50.2(3)	48.2(2)
Ir(1)–Ir(2)–P(2)	82.6(3)	88.5(3)	82.4(3)	102.7(2)
Ir(1)–Ir(2)–P(4)	99.8(2)	93.4(3)	104.4(3)	118.8(10)
Ir(1)–Ir(2)–C(4)	152.4(13)	148.2(11)	147.3(17)	105.8(11)
Ir(3)–Ir(2)–P(1)	111.9(2)	111.1(3)	111.8(3)	107.1(2)
Ir(3)–Ir(2)–P(2)	53.3(4)	54.0(3)	54.2(3)	44.4(2)
Ir(3)–Ir(2)–P(4)	93.4(2)	94.5(3)	91.5(3)	118.5(10)
Ir(3)–Ir(2)–C(4)	140.7(13)	146.6(10)	142.0(15)	100.3(10)
P(1)–Ir(2)–P(2)	107.6(4)	106.1(4)	115.0(5)	150.1(3)
P(1)–Ir(2)–P(4)	104.3(3)	102.4(4)	100.0(4)	96.8(10)
P(1)–Ir(2)–C(4)	102.5(13)	99.2(12)	102.8(16)	98.7(11)
P(2)–Ir(2)–P(4)	140.5(3)	143.4(4)	137.4(4)	92.6(10)
P(2)–Ir(2)–C(4)	99.3(12)	105.0(11)	97.4(16)	96.1(10)
P(4)–Ir(2)–C(4)	95.9(12)	92.4(12)	97.7(18)	131.2(14)
Ir(1)–Ir(3)–Ir(2)	60.7(1)	63.0(1)	63.7(1)	58.2(1)
Ir(1)–Ir(3)–P(2)	82.6(9)	88.2(3)	83.2(3)	101.8(2)
Ir(1)–Ir(3)–P(3)	51.7(2)	48.4(3)	51.4(3)	47.9(2)
Ir(1)–Ir(3)–P(5)	99.8(2)	104.3(3)	94.2(3)	113.6(11)
Ir(1)–Ir(3)–C(5)	152.4(13)	144.3(14)	160.2(19)	115.3(12)
Ir(2)–Ir(3)–P(2)	53.3(4)	54.6(3)	53.4(3)	44.2(2)
Ir(2)–Ir(3)–P(3)	111.9(2)	111.4(3)	113.7(3)	106.0(2)
Ir(2)–Ir(3)–P(5)	93.4(2)	90.5(3)	93.9(3)	117.8(11)
Ir(2)–Ir(3)–C(5)	140.7(13)	145.1(16)	133.3(16)	104.8(12)
P(2)–Ir(3)–P(3)	107.6(4)	117.2(4)	103.4(5)	149.4(3)
P(2)–Ir(3)–P(5)	140.5(3)	132.6(4)	144.7(4)	95.7(11)
P(2)–Ir(3)–C(5)	99.3(12)	97.2(17)	99.8(16)	93.6(11)
P(3)–Ir(3)–P(5)	104.3(3)	104.2(4)	102.2(4)	94.7(11)
P(3)–Ir(3)–C(5)	102.5(13)	99.3(15)	109.2(18)	102.9(11)
P(5)–Ir(3)–C(5)	95.9(12)	97.7(16)	94.3(19)	126.9(17)
Ir(1)–P(1)–Ir(2)	75.9(2)	82.9(4)	80.5(4)	86.2(2)
Ir(2)–P(2)–Ir(3)	73.5(4)	71.4(3)	72.4(4)	91.4(3)
Ir(1)–P(3)–Ir(3)	75.9(2)	83.3(4)	79.2(4)	86.3(2)
Ir(2)–P(4)–C(1)	114.9(13)	113.5(11)	111.5(16)	
Ir(3)–P(5)–C(1)	114.9(13)	113.2(13)	112.8(13)	
P(4)–C(1)–P(5)	109(2)	107.3(19)	106.2(18)	
Ir(1)–C(2)–O(2)	177(5)	169(3)	152(6)	180(3)
Ir(1)–C(3)–O(3)		163(4)	146(5)	
Ir(2)–C(4)–O(4)	174(3)	172(3)	180(4)	173(3)
Ir(3)–C(5)–O(5)	174(3)	172(5)	162(5)	176(4)

[a]e.s.d.s are given in parentheses. [b]Data from ref. 7.

are presented as average values throughout the following discussion.

The two molecules of **2** have approximately planar Ir_3–P(1)–P(3) cores, similar to that of **1**, with the angles between the Ir_3 planes and the Ir_2P planes ranging from 0 to 17°. In each molecule one phosphorus is almost in plane, the other slightly further out. The third PIr_2 triangle, P(2)–Ir(2)–Ir(3), is almost perpendicular to the metal plane, subtending an angle of 105° compared to 104° in **1**. In both **1** and **2** the dppm ligand spans the Ir(2,3) edge which is also bridged by the unique phosphorus, P(2). In **1**, the three carbonyl ligands are coordinated at the corners of the Ir_3 triangle, roughly coplanar with it, and **2** is similar except that at Ir(1) the single coplanar carbonyl of **1** is replaced by two carbonyls, above and below the metal plane, and subtending an angle of 87° to each other. Tables 2 and 3 show that the structural parameters of **2** are generally very similar to those of **1** except for the significant increase in the Ir(1)–Ir(2) and Ir(1)–Ir(3) distances, changing from 2.81 to 2.99 Å. At the same time, there is relatively little change in the Ir(2)–Ir(3) distance showing that the extra valence electrons are accommodated mainly at Ir(1). Somewhat surprisingly, the Ir(2)–Ir(3) distance actually decreases slightly from **1**, 2.74 Å, to **2**, 2.71 Å, but this is consistent with the NMR parameters as noted above. In **3** the Ir(2)–Ir(3) distance has increased to 3.33 Å. This lengthening may be partly attributable to the absence of the dppm bridge in **3** relative to **1** and **2**. However, the realignment of the P(2) bridge, coplanar with Ir_3–P(1)–P(2) in **3** but perpendicular to this plane in **1** and **2**, suggests that electronic factors associated with the increased electron count are probably more important.

Finally, we note that in compounds **1**–**3**, the Ir(1)–Ir(2) and Ir(1)–Ir(3) bond distances increase regularly, 2.81, 2.99 and 3.19 Å, as the valence electron count increases from 46 to 48 to 50 electrons. This is consistent with molecular orbital treatments such as that of Lauher [17], in which only 44 electrons are required to occupy all the bonding molecular orbitals of a triangular cluster. The next 6 electrons are accommodated in e″ and a_2' orbitals of anti-bonding character.

Supplementary material

For compound **2**: unit cell, data collection and refinement parameters, fractional atomic coordinates and isotropic temperature parameters for all atoms, anisotropic temperature factors for the heavy atoms, interatomic distances, bond angles, and selected intermolecular distances (Tables S1–S6, 14 pages); observed and calculated structure factor amplitudes (Table S7, 29 pages). These Tables are available from the authors and will also be deposited with the Cambridge Crystallographic Centre.

Acknowledgements

We thank the Natural Sciences and Engineering Research Council of Canada and the University of Victoria for research grants, Mrs K. Beveridge for technical assistance in the crystal structure determinations, and Mrs C. Greenwood for recording NMR spectra.

References

1 E. Billig, J.D. Jamerson and R.L. Pruett, *J. Organomet. Chem., 192* (1980) C49–51.
2 R.J. Haines, N.D.C.T. Steen and R.B. English, *J. Organomet. Chem., 209* (1981) C34–36.
3 R.J. Haines, N.D.C.T. Steen and R.B. English, *J. Chem. Soc., Chem. Commun.,* (1981) 407–408.
4 R.B. English, R.J. Haines and N.D. Steen, *J. Organomet. Chem., 238* (1982) C34–36.
5 J.L. Atwood, W.E. Hunter, R.A. Jones and T.C. Wright, *Inorg. Chem., 22* (1983) 993–995.
6 R.J. Haines, N.D.C.T Steen and R.B. English, *J. Chem. Soc., Dalton Trans.,* (1984) 515–525.
7 D.E. Berry, J. Browning, K. Dehghan, K.R. Dixon, N.J. Meanwell and A.J. Phillips, *Inorg. Chem., 30* (1991) 396–402.
8 A.M. Arif, D.E. Heaton, R.A. Jones, K.B. Kidd, T.B. Wright, B.R. Whittlesey, J.L. Atwood, W.E. Hunter and H. Zhang, *Inorg. Chem., 26* (1987) 4065–4073.
9 Y. Le Page, E.J. Gabe and P.S. White, *NRCCAD Modification of the ENRAF-NONIUS Program*, Chemistry Division, National Research Council of Canada, Ottawa, Canada.
10 D.F. Grant and E.J. Gabe, *J. Appl. Crystallogr., 11* (1978) 114–120.
11 A.C.T. North, D.C. Phillips and F.S. Mathews, *Acta Crystallogr., Sect. A, 24* (1968) 351–359.
12 G.M. Sheldrick, *SHELX-76*, a computer program for crystal structure determination, University of Cambridge, Cambridge, UK, 1976.
13 C.K. Johnson, ORTEP: a Fortran thermal ellipsoid plot program for crystal structure illustrations, *Rep. ORNL-3794*, Oak Ridge National Laboratory, Oak Ridge, TN, USA, 1965.
14 D.T. Cromer and J.T. Waber, in J.A. Ibers and W.C. Hamilton (eds.), *International Tables for X-Ray Crystallography*, Vol. IV, Kynoch, Birmingham, UK, 1974.
15 A.J. Carty, S.A. Maclaughlin and D. Nucciarone, in J.G. Verkade and L.D. Quin (eds.), *Phosphorus-31 NMR Spectroscopy in Stereochemical Analysis*, VCH, New York, 1987, pp. 559–620.
16 D.E. Berry. G.W. Bushnell, K.R. Dixon, P.M. Moroney and C. Wan, *Inorg. Chem., 24* (1985) 2625–2634.
17 J.W. Lauher, *J. Am. Chem. Soc., 100* (1978) 5305–5315.